Available online at http://scik.org
Commun. Math. Biol. Neurosci. 2024, 2024:109
https://doi.org/10.28919/cmbn/8873
ISSN: 2052-2541

ECO-EPIDEMIOLOGY OF LASSA FEVER: A MATHEMATICAL MODELING APPROACH

DELIGHT MAWUFEMOR AGBI[1], TÊLÉ JONAS DOUMATÈ[1,2], NICHOLAS KWASI-DO OHENE OPOKU[3], ROMAIN GLÈLÈ KAKAÏ[1,*]

[1]Laboratory of Biomathematics and Forest Estimation, University of Abomey-Calavi, Cotonou, Benin

[2]Department of Mathematics, Faculty of Sciences and Technics, University of Abomey-Calavi, Cotonou, Benin

[3]Department of Biochemistry and Biotechnology, Kwame Nkrumah University of Science and Technology, Kumasi, Ghana

Abstract. Lassa fever, a fatal zoonotic hemorrhagic disease caused by the Lassa virus, persists as a significant health concern in West Africa. Despite ongoing efforts to mitigate its impact, both the incidence and mortality rates remain alarmingly high, posing a potential risk of a global spread. Recent studies have focused on understanding the dynamic behaviour of Lassa fever. However, the ecological relationship between the reservoir host (rodents) and humans, involving factors such as rodent predation and migration, remains inadequately understood. In this study, we developed and analysed a non-linear mathematical compartmental model for Lassa fever, incorporating both human and rodent populations together with an infested environment. Rodent predation was modelled using the Holling type II functional response. We rigorously established key properties of the model, including the existence of solutions, boundedness, and positivity. The reproduction number (R_0) was determined using the next-generation method. Additionally, a sensitivity analysis of model parameters was conducted, utilising the Normalized Forward Sensitivity Index to identify the most influential processes affecting the disease threshold and critical factors for effective infection control. Numerical analysis of the total infected human population performed

*Corresponding author
E-mail address: romain.glelekakai@uac.bj
Received August 27, 2024

using the *odeint* function in Python programming revealed several insights. Notably, human-to-human transmission became predominant when the contact rate exceeded 50%. The infected human population experienced a drastic decline when the rate of rodent migration exceeded 50%. In addition, we observed that rodent predation led to an initial surge in human infections. The findings of this study underscore the importance of implementing strategies that prioritise minimising environmental transmission, human-to-human contact, mitigating rodent predation, and increasing rodent migration to effectively control and prevent the transmission of Lassa fever.

Keywords: Holling type II functional response; rodent predation; migration; sensitivity analysis.

2020 AMS Subject Classification: 92D30.

1. INTRODUCTION

Lassa fever (LF), a fatal zoonotic hemorrhagic infection, is a neglected tropical disease endemic in the West African countries of Benin, Ghana, Guinea, Liberia, Mali, Sierra Leone, and Nigeria. The widespread presence of the animal host suggests that all countries within the region are at risk of contracting the disease [1]. LF stands out among the numerous zoonotic diseases present in the African region due to its complex characteristics that interact to create a significant public health challenge. In 2015, the World Health Organization recognised the significance of LF and designated it among the list of "top priority pathogens" to prioritise for research and developmental activities due to its high mortality rate and epidemic potential. Since then, the disease has been included in subsequent lists of priority diseases published by WHO [2]. The annual incidence of LF stands at 300,000–500,000 cases with 5,000 deaths [3]. However, a recent modelled study [4] has shed new light on the burden of LF, predicting an estimated 897,700 to 4,383,600 individuals infected annually, revealing a far greater impact than previously estimated.

LF originated from the Nigerian town of Lassa in Borno State and was categorised as a viral hemorrhagic fever in 1969 following the tragic deaths of two missionary nurses [5]. The causative agent of LF is the Lassa virus (LASV), a member of the Arenaviridae family, which manifests in a range of clinical presentations. Rodents, especially the multimammate rat, harbour the LASV virus, and human infection often occurs through contact with rodent excreta or bodily fluids of infected individuals. The disease can also spread through contaminated food, the consumption of infected rodents, and exposure to virus particles (aerosol). Infections with

LF in humans trigger a broad spectrum of reactions, ranging from mild fever to severe hemorrhagic manifestations. According to the Centers for Disease Control and Prevention (CDC), the presentation of symptoms in LF can differ significantly among individuals. Approximately 80% of human LF cases display mild or undetectable symptoms, whereas the remaining 20% of cases experience severe manifestations, including respiratory problems, vomiting, and shock [6].

Mathematical modelling is central to infectious disease as it can create virtual environments to explore the detailed complexities underlying disease dissemination. Past mathematical modelling studies [7, 8, 9, 10, 11, 12, 13, 14, 4, 15, 16, 17, 18, 19] have made strides in providing insights into the transmission dynamics of LF and the potential impact of interventions and future outbreaks. Notably, studies have established that environmental factors, such as rainfall, relative humidity, temperature, and landscape, significantly influence the dynamics of virus circulation by altering the ecological suitability for its transmission [20]. Also, the migratory behaviour of rodents plays a crucial role, as these environmental conditions directly influence it [21, 22]. During the dry season, rodents migrate to areas near human settlements for breeding and hibernation, intensifying human-rodent contact and elevating the risk of LF transmission. This migration becomes a critical link in the chain of LF transmission, as the increased proximity between rodents and humans creates a higher probability of acquiring LF infection. Furthermore, socioeconomic and human behavioural factors, including demographics, education, occupation, and income, contribute significantly to the spread of LF [23]. Communities lacking essential amenities, grappling with malnutrition, residing in unclean environments, facing inadequate health facilities, and struggling with poor personal hygiene are particularly vulnerable to LF outbreaks. Also, rodent consumption behaviour by humans poses a significant threat to the incidence and spread of LF.

Despite the progress made, the ecological relationship between the human host and the animal vector (rodents) and its impact on LF transmission dynamics remain poorly understood. Therefore, this study aims to understand the transmission dynamics of LF in the ecological context of animal and human host interactions. Specifically, we want to know how intensified human predation on rodents influences the dynamics of Lassa fever transmission and what role

the migration of rodents plays in the disease's spread. To achieve this, we developed a simplified eco-epidemic model for LF that incorporates humans, rodents(rats) and ecological dimensions of disease transmission. The rest of this study is structured as follows: Section 2 describes the model formulation and assumptions. Section 3 covers model analysis, which includes establishing the basic properties of the model, the basic reproduction number, and sensitivity analysis. Section 4 focuses on numerical analysis, while Section 5 presents the conclusion and recommendations.

2. Mathematical Model Formulation and Assumptions

The formulated model considers two host populations: the human population $N_h(t)$ and the rodent population $N_r(t)$. The human host population is stratified into three mutually exclusive epidemiological classes: Susceptible humans (S_h), Infected humans (I_h), and Recovered humans (R_h), such that

$$N_h(t) = S_h(t) + I_h(t) + R_h(t). \tag{1a}$$

Similarly, the rodent population is stratified into Susceptible individuals $S_r(t)$ and infectious rodents $I_r(t)$ such that

$$N_r(t) = S_r(t) + I_r(t). \tag{1b}$$

In this model, the role of the environment in spreading the Lassa virus is taken into account. The concentration of Lassa virus pathogens found on surfaces or objects in the environment is represented by V (Figure 1). This occurs due to the shedding of the virus from infected individuals or mastomy rats. The model is formulated based on the following set of assumptions and considerations

A1 We assume logistic recruitment of rodents with an intrinsic growth rate b and an environmental carrying capacity k. Rodent recruitment was assumed to be constant, simplifying the analysis to a constant rate model. While this approach facilitates initial modeling, it is important to acknowledge that actual rodent populations are influenced by complex ecological factors, including variable birth and death rates. Consequently, the constant recruitment assumption may limit the model's predictive accuracy.

A2 In the presence of LF disease, susceptible humans become infected in three ways: a. while coming in contact with infected humans; b. while coming in contact with contaminated surfaces; c. while predating (hunting and consuming) infected rodents [24]. This study focuses on these pathways, however, it is essential to acknowledge the simplified nature of this model. Critical transmission dynamics, including aerosol transmission, the potential role of other wildlife reservoirs, and the nuanced differences between various human-to-human transmission contexts (e.g., household, hospital, mortuary), are not explicitly considered and this may significantly impact the conclusions and the generalizability of our findings.

A3 We assume that human predation on rodents, which serves as a transmission pathway for Lassa fever, follows a Michaelis-Menten kinetics model with a Holling type-II functional response. This model incorporates predation coefficients ($P_i > 0$, where $i = 1,2,3,4$), as well as a half-saturation constant $(a > 0)$ that represents the rodent density at which the predation rate is half of its maximum. Additionally, the model includes a handling time (h) that accounts for the time taken by humans to capture, consume, and process rodents, and an efficiency factor $(0 < q < 1)$ that represents the proportion of consumed rodents that are effectively converted into human energy or biomass[25].

A4 The contact rate between humans, rodents, and infected environment is assumed to follow a logistic-dose response curve, with η being the concentration of the Lassa virus in the environment. As reported by [11], this concentration increases the chance of triggering disease transmission by 50%.

A5 The human population has a constant recruitment rate Λ_h. Infected and recovered classes do not reproduce and arise only from susceptible and infected classes, respectively. Infected individuals can recover, but immunity is not permanent. Natural death reduces both human and rodent populations. The assumption of a constant recruitment rate for the human population however simplifies the dynamics of population changes by neglecting fluctuations due to factors such as migration, varying birth rates, and seasonal effects.

A6 The Human-to-human and rodent-to-rodent disease transmission is assumed to follow a standard incidence with the rates β_h and β_r, respectively. This indicates that the rate of new infections is proportional to the product of the number of susceptible and infectious individuals in each population. In essence, the more susceptible individuals there are in a population, and the more infected individuals there are, the higher the likelihood of disease transmission.

A7 We assume migration in rodent populations at the rates of m_1 and m_2, respectively. Also, ecology suggests that $m_1 > m_2$ as susceptible prey are stronger as compared to infected ones [26].This study assumes a constant rate of rodent migration, a simplification that streamlines model development. However, this static approach overlooks the complexity and dynamic nature of rodent movement, which is influenced by a complex interplay of environmental and biological factors.

According to the above assumptions, we have the following model flow diagram (Figure 1).

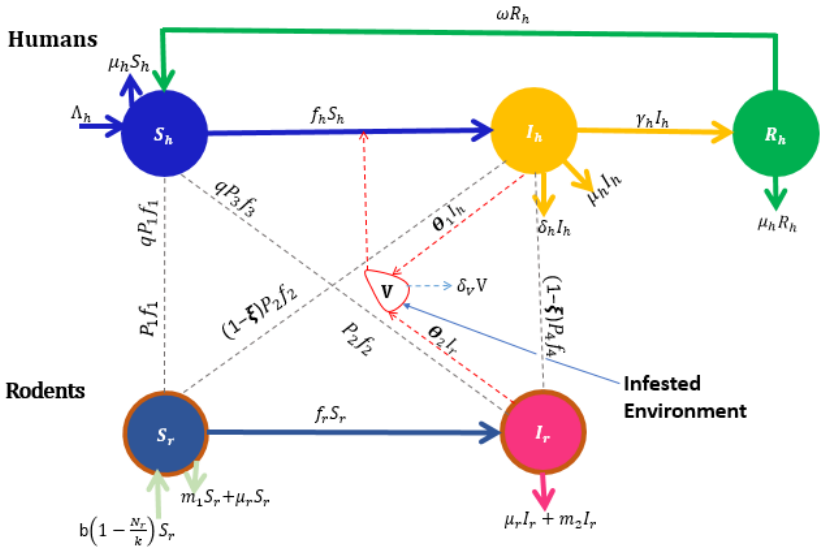

FIGURE 1. Flow diagram of Lassa fever transmission dynamics describing the interaction between humans and rodent population and virus-infested environment. Note: This study does not fully capture the transmission dynamics of LF.

with

$$f_r = \beta_r \frac{I_r}{N_r} + \beta_1 \frac{V}{\eta + V},\ f_h = \beta_h \frac{I_h}{N_h} + \beta_2 \frac{V}{\eta + V},\ f_1 = \frac{S_r S_h}{a + hS_r}, f_2 = \frac{S_r I_h}{a + hS_r}, f_3 = \frac{I_r S_h}{a + hI_r},\ f_4 = \frac{I_r I_h}{a + hI_r}.$$

From the model flow diagram in Figure 1, we have the following set of differential equations:

$$\text{(2a)} \quad \frac{dS_r}{dt} = b\left(1 - \frac{N_r}{k}\right) S_r - \frac{\beta_r S_r I_r}{N_r} - \frac{\beta_1 V S_r}{\eta + V} - \frac{P_1 S_r S_h}{a + hS_r} - (1 - \xi)\frac{P_2 S_r I_h}{a + hS_r} - (m_1 - \mu_r) S_r,$$

$$\text{(2b)} \quad \frac{dI_r}{dt} = \frac{\beta_r S_r I_r}{N_r} + \frac{\beta_1 V S_r}{\eta + V} - \frac{P_3 I_r S_h}{a + hI_r} - (1 - \xi)\frac{P_4 I_r I_h}{a + hI_r} - \mu_r I_r - m_2 I_r,$$

$$\text{(2c)} \quad \frac{dS_h}{dt} = \Lambda_h + \omega R_h - \frac{\beta_h S_h I_h}{N_h} - \frac{\beta_2 V S_h}{\eta + V} + q\frac{P_1 S_r S_h}{a + hS_r} + q\frac{P_3 S_h I_r}{a + hI_r} - \mu_h S_h,$$

$$\text{(2d)} \quad \frac{dI_h}{dt} = (1 - \xi) q \frac{P_2 S_r I_h}{a + hS_r} + (1 - \xi) q \frac{P_4 I_r I_h}{a + hI_r} + \frac{\beta_h S_h I_h}{N_h} + \frac{\beta_2 V S_h}{\eta + V} - (\gamma_h + \mu_h + \delta_h) I_h,$$

$$\text{(2e)} \quad \frac{dR_h}{dt} = \gamma_h I_h - \omega R_h - \mu_h R_h,$$

$$\text{(2f)} \quad \frac{dV}{dt} = \theta_1 I_h + \theta_2 I_r - \delta_v V.$$

with the initial conditions $S_r(0) > 0$; $I_r(0) \geq 0$; $S_h(0) > 0$; $I_h(0) \geq 0$; $R_h(0) \geq 0$; $V(0) \geq 0$ and all the parameters of the model are positive.

The state variables and parameters of the model are presented in Tables 1 and 2, respectively.

TABLE 1. Description of state variables of the Lassa fever model

State Variable	Description
S_r	Density of Susceptible rodents
I_r	Density of Infected rodents
S_h	Density of Susceptible humans
I_h	Density of Infected humans
R_h	Density of Recovered humans
V	Contaminated environments or surfaces with Lassa virus

TABLE 2. Description Parameters of the Lassa fever model

Parameters	Description
$b(\Lambda_h)$	Rate of recruitment of rodents (humans)
k	Environmental carrying capacity for rodent
$\beta_r(\beta_h)$	Disease transmission rate in rodents (humans)
$\beta_1(\beta_2)$	Rodent (Humans) contact rate with infested environment
δ_h	Disease-induced death rate in humans
$\mu_r(\mu_h)$	Rodents (Humans) natural death rates
γ_h	Recovery rate of infected humans
ω	Rate at which immunity wanes in humans after recovery
$m_1(m_2)$	Rate of migration of Susceptible (Infected) rodents
$\eta(\delta_v)$	LASV Concentration rate in the environment (virus decay)
$\theta_1(\theta_2)$	Virus shed in the environment by infected rodents (infected humans)
$q(a)$	Efficiency of rodent predation (Half saturation constant)
h	Rodent handling time by humans
ξ	Fraction of Symptomatic infectious humans
$P_1(P_2)$	Rate of predation of Susceptible Rodent by Susceptible(Infected) humans
$P_3(P_4)$	Rate of predation of Infected Rodent by Susceptible (Infected) humans

3. MAIN RESULTS

3.1. Basic properties of the model.

3.1.1. *Existence.*

Theorem 1. *Under assumptions on initial conditions, system* (2a)– (2f) *admits a unique global solution* $(S_r(t), I_r(t), S_h(t), I_h(t), R_h(t), V(t))$ *defined on* $\mathbb{R}^6$.

Proof. The Cauchy-Lipschitz theorem in [27] ensures the existence and uniqueness of a local (extended to global) solution to the system (2a)– (2f) on the interval $[0, T_{max}[$ given the regularity of the functions involved in the model.

3.1.2. *Boundedness.*

In theoretical eco-epidemiology, the boundedness of a system implies that the system is biologically valid and well-behaved. The following lemma ensures the boundedness of the system (2a)– (2f). Here, we prove that each of the subsystems—the rodent population, the human population, and the infested environment—is bounded.

Lemma 1. *All solutions of subsystem* (2a)– (2b) *that start in* $\mathbb{R}$ *are uniformly bounded within the region* $\Omega_r = (S_r, I_r) \in \mathbb{R}^2$*, where* $0 \leq N_r(t) \leq \frac{kb}{\mu_r}$

Proof. Let N_r represent the total rodent population such that $N_r = (S_r + I_r)$. Then,

$$\frac{dN_r}{dt} = \frac{dS_r}{dt} + \frac{dI_r}{dt}.$$

From the Equations (2a) – (2b),

$$\frac{dN_r}{dt} = b\left(1 - \frac{N_r}{k}\right)S_r - \frac{P_1 S_r S_h}{a + hS_r} - (1-\xi)\frac{P_2 S_r I_h}{a + hS_r} - (m_1 + \mu_r)S_r - \frac{P_3 I_r S_h}{a + hI_r} - (1-\xi)\frac{P_4 I_r I_h}{a + hI_r} - (\mu_r - m_2)I_r.$$

This implies that

$$\frac{dN_r}{dt} \leq b\left(1 - \frac{N_r}{k}\right)S_r - (m_1 + \mu_r)S_r - (\mu_r - m_2)I_r$$

$$\frac{dN_r}{dt} \leq bS_r - \mu_r S_r - \mu_r I_r$$

$$\frac{dN_r}{dt} \leq bS_r - \mu_r N_r$$

and since $S_r \leq k$, one can deduce that

$$\frac{dN_r}{dt} \leq bk - \mu_r N_r.$$

Now, applying the comparison principle for ODEs[28], we get

$$N_r(t) \leq e^{\int_0^t -\mu_r\, ds}\left[N_r(0) + \int_0^t e^{\int_0^\tau \mu_r dv}(bk)d\tau\right]$$

$$N_r(t) \leq e^{-\mu_r t}\left[N_r(0) + \int_0^t e^{\mu_r \tau}(bk)d\tau\right]$$

$$\leq e^{-\mu_r t}\left[N_r(0) + \frac{bk}{\mu_r}[e^{\mu_r t} - 1]\right]$$

$$\leq e^{-\mu_r t}N_r(0) + \frac{bk}{\mu_r} - \frac{bk}{\mu_r}e^{-\mu_r t}$$

$$N_r(t) \leq \frac{bk}{\mu_r} + \left(N_r(0) - \frac{bk}{\mu_r}\right) e^{-\mu_r t}.$$

As $t \to \infty$, $\quad N_r(t) \to \frac{bk}{\mu_r}$ and in consequence, $0 \leq N_r(t) \leq \frac{bk}{\mu_r}$. Hence, all solutions of the system will stay in the region $\Omega_r = (S_r, I_r) \in \mathbb{R}^2$ with $0 \leq N_r(t) \leq \frac{kb}{\mu_r}$.

In the following, we give proof of boundedness for the Human population.

Lemma 2. *All solutions of subsystem* (2c)– (2e) *that start in* $\mathbb{R}$ *are uniformly bounded within the region* $\Omega_h = (S_h, I_h, R_h) \in \mathbb{R}^3$ *where* $0 \leq N_h(t) \leq \frac{\Lambda_h}{\mu_h}$.

Proof. Let N_h be the total human population such that $N_h = (S_h + I_h + R_h)$. Then,

$$\frac{dN_h}{dt} = \frac{dS_h(t)}{dt} + \frac{I_h(t)}{dt} + \frac{R_h(t)}{dt}.$$

From the Equations (2c)– (2c),

$$\frac{dN_h}{dt} = \Lambda_h + q\frac{P_1 S_r S_h}{a + hS_r} + q\frac{P_3 S_h I_r}{a + hI_r} + (1-\xi)q\frac{P_2 S_r I_h}{a + hS_r} + (1-\xi)q\frac{P_4 I_r I_h}{a + hI_r} - \delta_h I_h - \mu_h R_h$$
$$-\mu_h S_h - \mu_h I_h$$

which yields

$$\frac{dN_h(t)}{dt} \leq \Lambda_h - \delta_h I_h - \mu_h R_h - \mu_h S_h - \mu_h I_h$$
$$\frac{dN_h(t)}{dt} \leq \Lambda_h - \delta_h I_h - (S_h + I_h + R_h)\mu_h$$
$$\leq \Lambda_h - N_h \mu_h.$$

We can now invoke the comparison principle for ODEs to conclude that

$$N_h(t) \leq e^{\int_0^t -\mu_h \, ds}\left[N_h(0) + \int_0^t e^{\int_0^\tau \mu_h dv}(\Lambda_h) d\tau\right]$$
$$N_h(t) \leq e^{-\mu_h t}\left[N_h(0) + \int_0^t e^{\mu_h \tau}(\Lambda_h) d\tau\right]$$
$$\leq e^{-\mu_h t}\left[N_h(0) + \frac{\Lambda_h}{\mu_h}[e^{\mu_h t} - 1]\right]$$
$$\leq e^{-\mu_h t} N_h(0) + \frac{\Lambda_h}{\mu_h} - \frac{\Lambda_h}{\mu_h} e^{-\mu_h t}$$
$$N_h(t) \leq \frac{\Lambda_h}{\mu_h} + \left(N_h(0) - \frac{\Lambda_h}{\mu_h}\right) e^{-\mu_h t}.$$

Letting $t \to \infty$, we have $N_h(t) \to \frac{\Lambda_h}{\mu_h}$ and then $0 \leq N_h(t) \leq \frac{\Lambda_h}{\mu_h}$.

The following result proves the boundedness of contaminated surfaces or environments.

Lemma 3 *All solutions of subsystem* (2f) *that start in* $\mathbb{R}$ *are uniformly bounded within the region* $\Omega_v = (V) \in \mathbb{R}$*, where* $0 \leq N_V \leq \frac{1}{\delta_v}\left(\theta_1 \frac{\Lambda_h}{\mu_h} + \theta_2 \frac{kb}{\mu_r}\right)$.

Proof. Let N_v be the total contaminated surfaces or environment, such that $N_v = V$. Then,

$$\frac{dN_v}{dt} = \frac{dV}{dt}.$$

From the Equations (2f),

$$\frac{dN_v}{dt} = \theta_1 I_h + \theta_2 I_r - \delta_v V$$

$$\leq \theta_1 I_h + \theta_2 I_r - \delta_v N_v.$$

From Lemmas 1 and 2, we have already established that the state variables I_r and I_h are bounded. Thus, $0 \leq I_h \leq \frac{\Lambda_h}{\mu_h}$ and $0 \leq I_r \leq \frac{kb}{\mu_r}$. Therefore,

$$\frac{dN_v}{dt} \leq \theta_1 \frac{\Lambda_h}{\mu_h} + \theta_2 \frac{kb}{\mu_r} - \delta_v N_v$$

Using a similar argument as in previous lemmas, we get

$$N_v(t) \leq e^{\int_0^t -\delta_v ds}\left[N_v(0) + \int_0^t e^{\int_0^\tau \delta_v dv}\left(\theta_1 \frac{\Lambda_h}{\mu_h} + \theta_2 \frac{kb}{\mu_r}\right) d\tau\right]$$

$$N_v(t) \leq e^{-\delta_v t}\left[N_v(0) + \left(\theta_1 \frac{\Lambda_h}{\mu_h} + \theta_2 \frac{kb}{\mu_r}\right) \int_0^t e^{\delta_v \tau} d\tau\right]$$

$$N_v(t) \leq e^{-\delta_v t}\left[N_h(0) + \left(\theta_1 \frac{\Lambda_h}{\mu_h} + \theta_2 \frac{kb}{\mu_r}\right) \frac{1}{\delta_v}[e^{\delta_v \tau}]_0^t\right]$$

$$\leq e^{-\mu_h t}\left[N_v(0) + \left(\theta_1 \frac{\Lambda_h}{\mu_h} + \theta_2 \frac{kb}{\mu_r}\right) \frac{1}{\delta_v}[e^{\mu_h t} - 1]\right]$$

$$\leq e^{-\delta_v t} N_v(0) + \left(\theta_1 \frac{\Lambda_h}{\mu_h} + \theta_2 \frac{kb}{\mu_r}\right) \frac{1}{\delta_v} - \left(\theta_1 \frac{\Lambda_h}{\mu_h} + \theta_2 \frac{kb}{\mu_r}\right) \frac{1}{\delta_v} e^{-\delta_v t}$$

$$\leq \left(\theta_1 \frac{\Lambda_h}{\mu_h} + \theta_2 \frac{kb}{\mu_r}\right) \frac{1}{\delta_v} + \left(N_v(0) - \left(\theta_1 \frac{\Lambda_h}{\mu_h} + \theta_2 \frac{kb}{\mu_r}\right) \frac{1}{\delta_v}\right) e^{-\delta_v t}.$$

We then conclude as t goes to ∞ that $0 \leq N_v(t) \leq \frac{1}{\delta_v}\left(\theta_1 \frac{\Lambda_h}{\mu_h} + \theta_2 \frac{kb}{\mu_r}\right)$ and consequently, all solutions of the system will stay in the region $\Omega_V = V \in \mathbb{R}$ satisfying $0 \leq N_V \leq \frac{1}{\delta_v}\left(\theta_1 \frac{\Lambda_h}{\mu_h} + \theta_2 \frac{kb}{\mu_r}\right)$.

Remark 1. *From the result of boundedness of solutions, one can state that the set* $\Omega = \Omega_h \times \Omega_r \times \Omega_V$ *is an invariant and absorbing set for system* (2a)– (2f) *together with its initial conditions, where*

$$\Omega_h = \left\{\Omega_r = \left\{(S_r, I_r) \in \mathbb{R}^2_+\right\}, \quad (S_h, I_h, R_h) \in \mathbb{R}^3_+\right\}, \quad \Omega_V = \left\{(V) \in \mathbb{R}^1_+\right\} \text{ such that,}$$

$$\left\{0 \leq N_r(t) \leq \frac{kb}{\mu_r}, 0 \leq N_h(t) \leq \frac{\Lambda_h}{\mu_h}, 0 \leq V(t) \leq \left(\theta_1 \frac{\Lambda_h}{\mu_h} + \theta_2 \frac{kb}{\mu_r}\right) \frac{1}{\delta_v}\right\}$$

is positive invariant.

3.1.3. *Positivity of solutions.* **Theorem 2.** *All solutions of the model* (2a)– (2f) *with initial conditions are positive for all time* t.

Proof. To prove this theorem, we shall show that each variable $S_r, I_r, S_h, I_h, R_h, V$ of the model (2a)– (2f) is nonnegative for all $t \geq 0$. From equation (2a) and after removing all the positive terms from the right-hand side of the differential equation, we have the following differential inequality:

$$\frac{dS_r}{dt} \geq -\left(\frac{bS_r^2 + bS_r I_r}{k} + \beta_r \frac{S_r I_r}{N_r} + \beta_1 \frac{VS_r}{\eta + V} + \frac{P_1 S_r S_h + (1-\xi) P_2 S_r I_h}{a + hS_r} + m_1 S_r + \mu_r S_r\right).$$

Then,

$$-\frac{dS_r}{dt} \leq S_r \left(bS_r + bI_r + \beta_r I_r + \beta_1 V + P_1 S_h + (1-\xi) P_2 I_h + m_1 + \mu_r\right).$$

Let $Q_1 = bI_r + \beta_r I_r + \beta_1 V + P_1 S_h + (1-\xi) P_2 I_h + m_1 + \mu_r$. Then, the inequality becomes

$$-\left(\frac{dS_r}{dt}\right) \leq S_r \left(bS_r + Q_1\right)$$

and one can write

$$\int \frac{1}{S_r \left(bS_r + Q_1\right)} dS_r \geq -\int dt.$$

By partial fraction decomposition, we have

$$\int \frac{1}{Q_1 S_r} dS_r + \int \frac{-b/Q_1}{bS_r + Q_1} dS_r \geq -\int dt.$$

Hence,

$$S_r(t) \geq \frac{AQ_1 e^{-Q_1 t}}{1 - Abe^{-Q_1 t}} \quad \text{where,} \quad A = e^{Q_1 Q_2}.$$

We can conclude that $S_r(t)$ is positive for all $t > \frac{1}{Q_1} \ln(bA)$ given that $Q_1 > 0$, $b > 0$, and $A > 0$. From the above proof, we have demonstrated that $S_r(t) > 0$, for all $t \geq 0$, then, we can generalise

that all the other variables in the model (2b)– (2f); $I_r(t)$, $S_h(t)$, $I_h(t)$, $R_h(t)$ and $V(t)$) are also positive for the same time interval.

3.2. Mathematical analysis of the model.

Disease-Free Equilibrium States. The disease-free equilibrium (DFE) state of the model occurs when there is no Lassa fever infection. Thus, in the absence of Lassa fever in the system given by equations (2a) – (2f), the variables related to infection (I_r, I_h, R_h, and V) can be set to zero. This simplifies the model, reducing equations (2a) – (2f) to the following:

$$bS_r\left(1-\frac{S_r}{k}\right)-P_1\frac{S_rS_h}{a+hS_r}-(m_1+\mu_r)S_r=0 \tag{3a}$$

$$\Lambda_h+qP_1\frac{S_rS_h}{a+hS_r}-\mu_hS_h=0. \tag{3b}$$

Due to the mathematical complexity of equations (3a) –(3b), we solve the equations by making assumptions. We consider different cases to facilitate the solvability.

3.2.1. *Case where there is no hunting and consumption of rodents (no preying).* Here, we assume humans are not predating on rodents as such, the rate of predation $P=0$. This assumption is grounded in specific socio-cultural and regulatory factors. The rationale for adopting this assumption stems from established rules and regulations in certain communities that explicitly prohibit the hunting and butchering of rodents [29]. Solving the equations (3a)– (3b) for S_r and S_h, we obtain the equilibrium point,

$$S_r=\tilde{S}_r=k\left(1-\frac{m_1+\mu_r}{b}\right) \tag{4a}$$

$$S_h=\tilde{S}_h=\frac{\Lambda_h}{\mu_h}. \tag{4b}$$

3.2.2. *Case where the rate of predation of susceptible rodents is greater than zero but the predation efficiency is zero (useless preying).* In this context where $P_1>0$ and $q=0$, we assume the existence of a certain degree of humans predating on rodents. However, the efficiency of predation is zero. Assuming $h>0$, one obtains from equation (3a):

$$S_r^2-\left(\tilde{S}_r-\frac{a}{h}\right)S_r-\frac{1}{h}\left(a\tilde{S}_r-\frac{P_1k}{b}S_h\right)=0. \tag{5a}$$

This gives:

$$S_r = \frac{1}{2}\left[\tilde{S}_r - \frac{a}{h} \pm \sqrt{\Delta_0}\right] \tag{5b}$$

$$S_h = \tilde{S}_h. \tag{5c}$$

where $\Delta_0 = \left(\tilde{S}_r - \frac{a}{h}\right)^2 + \frac{4}{h}\left[a\tilde{S}_r - \frac{P_1 K}{b} S_h\right] = \left(\tilde{S}_r + \frac{a}{h}\right)^2 - \frac{4P_1 k}{hb} S_h$. Subsequently, the number of equations depends on the values of Δ_0:

- If $\Delta_0 = 0$, a singular solution exists.
- If $\Delta_0 > 0$, two solutions emerge.
- If $\Delta_0 < 0$, no solutions are found.

Substituting $\Delta_0 = 0$ into (5b), we have:

$$S_r = \frac{1}{2}\left[\tilde{S}_r - \frac{a}{h} \pm \sqrt{\Delta_0}\right] = \quad \frac{1}{2}\left[\tilde{S}_r - \frac{a}{h}\right]. \tag{5d}$$

Subsequently, S_h and S_r are given as follows:

$$S_r = \frac{1}{2}\left[\tilde{S}_r - \frac{a}{h}\right] \tag{5e}$$

$$S_h = \tilde{S}_h. \tag{5f}$$

For $\Delta_0 > 0$, the solutions for S_r are given by:

$$S_r = \frac{1}{2}\left[\tilde{S}_r - \frac{a}{h} + \sqrt{\Delta_0}\right] \tag{5g}$$

$$S_r = \frac{1}{2}\left[\tilde{S}_r - \frac{a}{h} - \sqrt{\Delta_0}\right]. \tag{5h}$$

3.2.3. *Case where the rate of predation of susceptible rodents is greater than zero (useful preying).* In this particular scenario where $qP_1 > 0$, we assume active and successful predation of susceptible rodents by susceptible humans. This assumption finds its rationale in communities where humans engage in the active and successful hunting and butchering of rodents. Unlike the preceding case, the reasons behind this active predation are multifaceted. According to [30], hunting holds a significant cultural role as it represents not only a means of sustenance but a deeply ingrained tradition. Additionally, the difficulty in accessing conventional meat sources due to factors such as scarcity and poverty propels communities to actively pursue rodents as supplementary food sources.

Solving equation (3b) for $P_1\frac{S_rS_h}{a+hS_r}$ to get $P_1\frac{S_rS_h}{a+hS_r} = \frac{1}{q}(\mu_h S_h - \Lambda_h)$. The latter is thus a constant (not a function of S_r). We substitute it into equation (3a) to obtain:

$$S_r^2 - \tilde{S}_r S_r + \frac{k}{qb}(\mu_h S_h - \Lambda_h) = 0. \tag{6a}$$

Setting $\Delta_q = \tilde{S}_r^2 - 4\frac{k}{qb}(\mu_h S_h - \Lambda_h)$, we have S_r as a function of S_h:

$$S_r = \frac{1}{2}\left(\tilde{S}_r \pm \sqrt{\Delta_q}\right). \tag{6b}$$

Now we can feed (6b) back into (3b) to obtain one equation in S_h only. This would lead to an equation of degree 1.5. We can instead write both S_r and S_h in terms of Δ_q to have a third-degree polynomial in $x = \sqrt{\Delta_q}$ ($x \geq 0$) i.e., from equation (6b), $k \in \{-1, 1\}$,

$$S_r = \frac{1}{2}\left(\tilde{S}_r + kx\right) \quad \text{and} \tag{6c}$$

$$S_h = \tilde{S}_h + \frac{qb}{4\mu_h k}\left(\tilde{S}_r^2 - x^2\right), \tag{6d}$$

we can successively write

$$\Lambda_h(a + hS_r) + qP_1 S_r S_h - \mu_h S_h(a + hS_r) = 0 \tag{6e}$$

$$\Lambda_h(a + hS_r) + (qP_1 - h\mu_h) S_r S_h - a\mu_h S_h = 0. \tag{6f}$$

We can here distinguish two cases: $qP_1 - h\mu_h = 0$ and $qP_1 - h\mu_h \neq 0$.

Case $q\frac{P_1}{h} = \mu_h$: The equilibrium between successful predation rates over time and natural human death rates suggests a stable state, indicating that humans are likely controlling rodent populations at a rate similar to human mortality. This implies the potential for a relatively stable rodent population over time.

From equation (6f), we have $\mu_h S_h - \Lambda_h = \frac{h\Lambda_h}{a} S_r$, which plug back into (6a) leads to

$$S_r = \tilde{S}_r - \frac{hk\Lambda_h}{aqb} \quad \text{and} \tag{7a}$$

$$S_h = \tilde{S}_h\left(1 + \frac{h}{a}S_r\right). \tag{7b}$$

Case $q\frac{P_1}{h} \neq \mu_h$: Here, the total predation rate of humans on rodents is not equal to the natural death rate of humans. From equation (6f), we have the cubic (in x):

$$\begin{aligned}\Lambda_h\left(a+\frac{h}{2}\left(\tilde{S}_r+kx\right)\right)-a\mu_h\left[\tilde{S}_h+\frac{qb}{4\mu_h k}\left(\tilde{S}_r^2-x^2\right)\right]\\ +\frac{1}{2}\left(qP_1-h\mu_h\right)\left(\tilde{S}_r+kx\right)\left[\tilde{S}_h+\frac{qb}{4\mu_h k}\left(\tilde{S}_r^2-x^2\right)\right]=0.\end{aligned} \tag{8}$$

One can use Cardano's formula as applied in [31, 32] to solve (8).

3.3. Reproduction number and local stability of DFE.

The basic reproduction number (R_0) is an important parameter used to study the behaviour of epidemiological models. It is defined as the average number of secondary infections infected by an infective individual during an infective period, provided that all members of the population are susceptible. If $R_0 < 1$, then on average, an infected individual produces less than one new infected individual throughout its infectious period, and the infection cannot grow. Conversely, if $R_0 > 1$, then each infected individual produces, on average, more than one new infection, and the disease can invade the population. Here, following the approaches of [33, 13], we applied the next-generation matrix technique to obtain the basic reproduction number for Lassa fever disease.

GENERAL CASE

Let I denote the vector of the compartments involving infected individuals/material: $I = (I_r, I_h, V)$. The corresponding subset of the LF model has the form $\dot{I} = \mathbb{F}(I) - \mathbb{W}(I)$ where

$$\mathbb{F}(I) = \begin{pmatrix} \left(\beta_r \frac{I_r}{N_r} + \beta_1 \frac{V}{\eta+V}\right) S_r \\ \left(\beta_h \frac{I_h}{N_h} + \beta_2 \frac{V}{\eta+V}\right) S_h + (1-\xi) q P_2 \frac{I_h}{a+hS_r} S_r \\ 0 \end{pmatrix} \text{ and}$$

$$\mathbb{W}(I) = \begin{pmatrix} \left(P_3 \frac{S_h}{a+hI_r} + (1-\xi) P_4 \frac{I_h}{a+hI_r} + g_r\right) I_r \\ \left(-(1-\xi) q P_4 \frac{I_r}{a+hI_r} + g_h\right) I_h \\ -\theta_1 I_h - \theta_2 I_r + g_v V \end{pmatrix}.$$

with $g_r = \mu_r + m_2$, $g_h = \gamma_h + \mu_h + \delta_h$ and $g_v = \delta_v$.

The Jacobian matrices of $\mathbb{F}$ and $\mathbb{W}$ evaluated at the DFE are respectively given by

$$F = \begin{pmatrix} \beta_r & 0 & \beta_1 \frac{S_r}{\eta} \\ 0 & \beta_h + (1-\xi) q P_2 \frac{S_r}{a+hS_r} & \beta_2 \frac{S_h}{\eta} \\ 0 & 0 & \end{pmatrix} \text{ and}$$

$$W = \begin{pmatrix} \frac{P_3 S_h}{a} + g_r & 0 & 0 \\ 0 & g_h & 0 \\ -\theta_2 & -\theta_1 & g_v \end{pmatrix}.$$

The basic reproduction number $\mathscr{R}_0$ is defined as the spectral radius s_ρ (largest eigenvalue) of the next-generation matrix FW^{-1}. We have

$$W^{-1} = \frac{1}{g_h g_v \left(\frac{P_3 S_h}{a} + g_r\right)} \begin{pmatrix} g_h g_v & 0 & 0 \\ 0 & \left(\frac{P_3 S_h}{a} + g_r\right) g_v & 0 \\ -\theta_2 g_h & -\theta_1 \left(\frac{P_3 S_h}{a} + g_r\right) & g_h \left(\frac{P_3 S_h}{a} + g_r\right) \end{pmatrix}$$

Because the last row of F is null, we can ignore the last row and column of the next-generation matrix FW^{-1} to obtain:

$$\mathscr{R}_0 = s_\rho \left(FW^{-1}\right) = \frac{1}{g_h g_v \left(\frac{P_3 S_h}{a} + g_r\right)} s_\rho(Q) \quad \text{where}$$

$$Q = \begin{pmatrix} \beta_r g_h g_v - \beta_1 \frac{S_r}{\eta} \theta_2 g_h & -\beta_1 \frac{S_r}{\eta} \theta_1 \left(\frac{P_3 S_h}{a} + g_r\right) \\ -\beta_2 \frac{S_h}{\eta} \theta_2 g_h & \left[\beta_h + (1-\xi) q P_2 \frac{S_r}{a+hS_r}\right] \left(\frac{P_3 S_h}{a} + g_r\right) g_v - \beta_2 \frac{S_h}{\eta} \theta_1 \left(\frac{P_3 S_h}{a} + g_r\right) \end{pmatrix}.$$

that is

$$\mathscr{R}_0 = \frac{1}{2 g_h g_v \left(\frac{P_3 S_h}{a} + g_r\right)} \left(Q_{11} + Q_{22} + \sqrt{(Q_{11} - Q_{22})^2 + 4 Q_{12} Q_{21}}\right). \tag{9}$$

Having solved the Disease-Free Equilibrium (DFE) equation under various assumptions, we used the derived equilibrium points to determine specific reproduction numbers from the general number. Our specific focus lies on the equilibrium points acquired under two conditions: one where we assumed no predation ($p = 0$) and another where there is efficient predation on rodents ($P > 0$ and $q = 0$). We opt to work exclusively with these two cases as they offer a more intuitive understanding, providing valuable insights into the behaviour of our system when there is and isn't predation.

Remark 2. Note that the linearized system at DFE is always cooperative and based on [34,

Theorem 2.], the DFE of the model is locally asymptotically stable if $\mathscr{R}_0 < 1$ and unstable if $\mathscr{R}_0 > 1$. The question of uniqueness and global stability turns out to be challenging due to the complexity of our model, and we plan to explore these questions further in future works.

3.3.1. *Basic reproduction number: Case where there is no hunting and consumption of rodents.* The basic reproduction number is expressed for the case where there is no predation of susceptible rodents ($P_1 = 0$) as:

$$\mathscr{R}_0 = \frac{1}{2g_h g_v\left(\frac{P_3 S_h}{a} + g_r\right)}\left(Q_{11} + Q_{22} + \sqrt{(Q_{11} - Q_{22})^2 + 4Q_{12}Q_{21}}\right) \tag{10}$$

where

$$Q11 = \beta_r g_h g_v - \beta_1 \frac{S_r}{\eta}\theta_2 g_h$$

$$Q12 = -\beta_1 \frac{S_r}{\eta}\theta_1\left(\frac{P_3 S_h}{a} + g_r\right)$$

$$Q21 = -\beta_2 \frac{S_h}{\eta}\theta_2 g_h$$

$$Q22 = \left[\beta_h + (1-\xi)qP_2\frac{S_r}{a+hS_r}\right]\left(\frac{P_3 S_h}{a} + g_r\right)g_v - \beta_2\frac{S_h}{\eta}\theta_1\left(\frac{P_3 S_h}{a} + g_r\right)$$

$$S_r = k\left(1 - \frac{m_1 + \mu_r}{b}\right), S_h = \frac{\Lambda_h}{\mu_h}, g_r = \mu_r + m_2, g_h = \gamma_h + \mu_h + \delta_h, g_v = \delta_v.$$

3.3.2. *Basic reproduction number: Case where there is efficient hunting and consumption (predation) of rodents.* The basic reproduction number for case where $\frac{qP_1}{h} = \mu_h$ is expressed as:

$$\mathscr{R}_0 = \frac{1}{2g_h g_v\left(\frac{P_3 S_h}{a} + g_r\right)}\left(Q_{11} + Q_{22} + \sqrt{(Q_{11} - Q_{22})^2 + 4Q_{12}Q_{21}}\right) \tag{11}$$

where

$$Q11 = \beta_r g_h g_v - \beta_1 \frac{S_r}{\eta}\theta_2 g_h$$

$$Q12 = -\beta_1 \frac{S_r}{\eta}\theta_1\left(\frac{P_3 S_h}{a} + g_r\right)$$

$$Q21 = -\beta_2 \frac{S_h}{\eta}\theta_2 g_h$$

$$Q22 = \left[\beta_h + (1-\xi)qP_2\frac{S_r}{a+hS_r}\right]\left(\frac{P_3 S_h}{a} + g_r\right)g_v - \beta_2\frac{S_h}{\eta}\theta_1\left(\frac{P_3 S_h}{a} + g_r\right)$$

$$S_r = k\left(1-\frac{m_1+\mu_r}{b}\right)-\frac{hk\Lambda_h}{aqb}, \quad S_h = \frac{\Lambda_h}{\mu_h}\left(1+\frac{h}{a}S_r\right), g_r = \mu_r + m_2, g_h = \gamma_h + \mu_h + \delta_h, g_v = \delta_v.$$

3.4. Sensitivity Analysis.

Sensitivity analysis was performed to explore parameters that contribute to the variability of the Lassa fever infection, using the basic reproduction number as an index case. To determine which parameters highly influence the reproduction number and following the approach in [35], we performed the Forward Normalized Sensitivity Index (FNSI) implemented in the Python programming language.

Definition 1. *Let R_0 be the reproduction number, which is a function dependent on a set of parameters, Z_i. The sensitivity index of Z_i relative to R_0 is defined as follows:*

$$\Gamma_{R_0}^{Z_i} = \frac{\partial R_0}{\partial Z_i} \times \frac{Z_i}{R_0}.$$

For our system, recall that the reproduction number is computed for cases where we assumed that there is no predation on rodents at the DFE ($P = 0$) and the case where both there is efficient predation ($P > 0$ and $q > 0$). Therefore, the sensitivity analysis is conducted for the two separate reproduction numbers. The sensitivity indices are calculated and presented in Tables 4 and 5. Additionally, visualisations in the form of tornado plots for the normalised sensitivity index are presented in Figures 3 and 4.

3.4.1. *Sensitivity analysis conducted for the reproduction number in the absence of rodent predation.* Table 3 presents the sensitivity values of R_0 for the case where $P = 0$. Parameters with positive indices will increase the reproduction number (R_0) when they are increased, while parameters with negative NFSI values will decrease (R_0) when they are increased. We observe that the rate of predation of infected rodents by susceptible humans (P_3), handling time (h), virus decay rate (δ_v), recovery rate of humans (γ_h), human recruitment rate (Λ_h), disease-induced death rate (δ_h), predation of susceptible rodents by infected humans (P_2), saturation constant (a), and natural death rate of humans (μ_h) are most sensitive to (R_0). This implies that when the parameters with negative values (P_3,h,δ_v,γ_h,δ_h,Λ_h) are increased, the rate at which the disease would be transmitted from one individual to another will decrease, leading to a corresponding decrease in the basic reproduction number (R_0). Similarly, increasing the value of parameters

with positive values (P_2,a,q, μ_h) implies that the rate at which the disease would be transmitted from one individual to another will increase, leading to a corresponding increase in the basic reproduction number (R_0).

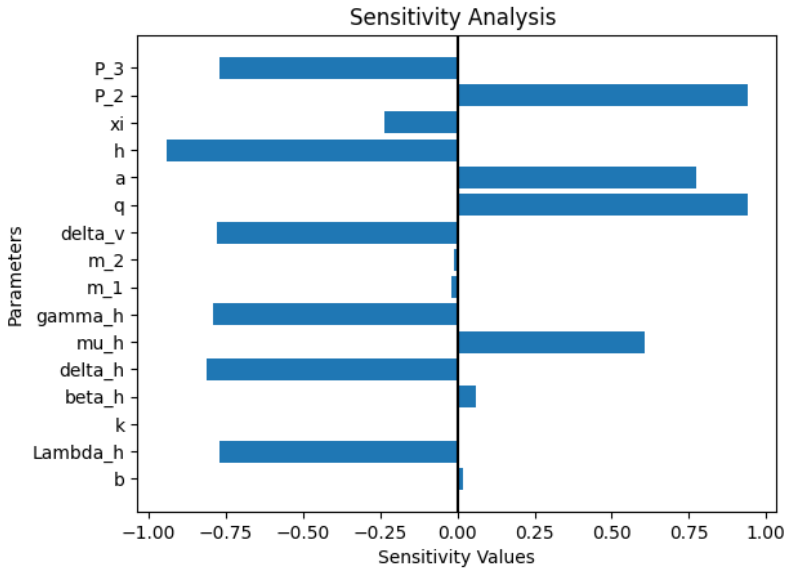

FIGURE 2. Sensitivity indices for R_0 in Case $P = 0$ with respect to each system parameter

TABLE 3. Sensitivity of R_0 to system parameters

Parameter	Description	Sensitivity Value
b	Recruitment rate of rodents	0.018
Λ_h	Recruitment rate of humans	-0.771
k	Environmental carrying capacity for rodent	-0.003
β_r	Disease transmission rate in rodents	-0.000
β_h	Disease transmission rate in humans	0.060
β_1	Rodents contact rate with infested environment	-0.000
β_2	Humans contact rate with infested environment	-0.000
δ_h	Disease-induced death rate in humans	-0.811
μ_r	Humans natural death rate	-0.000
μ_h	Rodents natural death rate	0.609
γ_h	Recovery rate of infected humans	-0.790
m_1	Rate of migration by Susceptible rodents	-0.018
m_2	Rate of migration by Infected rodents	-0.010
η	Rate of Lassa virus Concentration in the environment	0.000
δ_v	Rate of Lassa virus decay from the environment	-0.780
θ_1	Rate of virus shed in the environment by infected humans	-0.000
θ_2	Rate of virus shed in the environment by infected rodents	-0.000
q	Efficiency of predation	0.940
a	Half saturation constant	0.773
h	Rodent handling time by humans	-0.943
ξ	Fraction of Symptomatic infectious humans	-0.235
P_2	Rate of predation of Susceptible Rodent by Infected humans	0.940
P_3	Rate of predation of Infected Rodent by Susceptible humans	-0.771
R_0	**Basic reproduction number**	**2.165**

3.4.2. *Sensitivity analysis conducted for the reproduction number under conditions of efficient rodent predation.* Table 3 presents the sensitivity values of R_0 for the case where $\frac{qP_1}{h} = \mu_h$. Similar to the interpretation of Table 3, in Table 4, parameters with positive normalised sensitivity values will increase the reproduction number (R_0) when they are increased, while parameters with negative sensitivity values will decrease the reproduction number (R_0) when they are increased. We observe that the predation of infected rodents by susceptible humans (P_3), handling time (h), virus decay rate (δ_v), migration rate of susceptible and infected rodents (m_1, m_2), recovery rate of humans (γ_h), human recruitment rate (Λ_h), disease-induced death rate (δ_h), predation of susceptible rodents by infected humans (P_2), saturation constant (a), and natural death rate of humans (m_1) are most sensitive to (R_0). This implies that when the parameters with negative values (P_3,h,δ_v,m_2,γ_h,Λ_h) are increased, the rate at which the disease would be transmitted from one individual to another will decrease, leading to a corresponding decrease in the basic reproduction number (R_0). Similarly, increasing the value of parameters with positive values (P_2,a,q, m_1) implies that the rate at which the disease would be transmitted from one individual to another will increase, leading to a corresponding increase in the basic reproduction number (R_0).

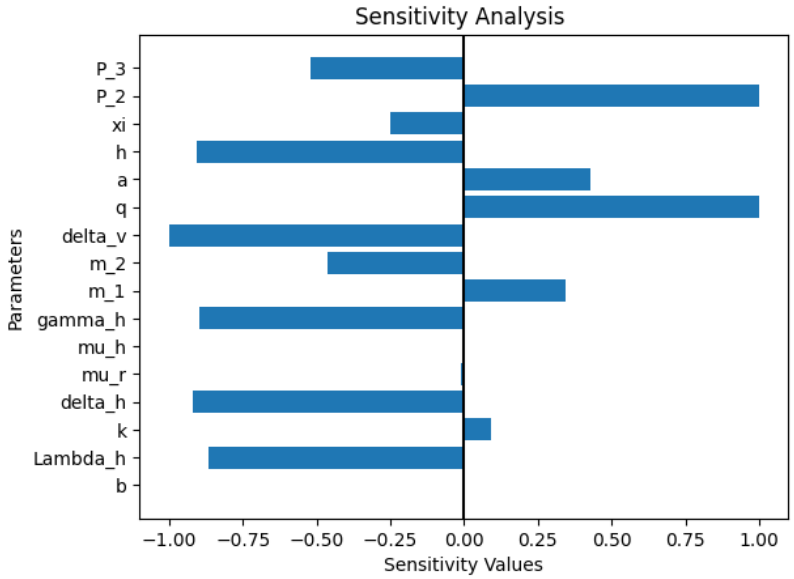

FIGURE 3. Sensitivity indices for R_0 in Case $P > 0$ and $q > 0$ with respect to each system parameter

TABLE 4. Sensitivity of the R_0 to system parameters

Parameter	Description	Sensitivity Value
b	Recruitment of rodents	-0.001
Λ_h	Recruitment of humans	-0.866
k	Environmental carrying capacity for rodent	0.091
β_r	Disease transmission rate in rodents	-0.000
β_h	Disease transmission rate in humans	0.000
β_1	Rodent contact rate with infested environment	-0.000
β_2	Humans contact rate with infested environment	0.000
δ_h	Disease-induced death rate in humans	-0.920
μ_r	Humans natural death rate	-0.012
μ_h	Rodents natural death rate	-0.00754
γ_h	Recovery rate of infected humans	-0.897
m_1	Rate of migration by Susceptible rodents	0.344
m_2	Rate of migration by Infected rodents	-0.464
η	Rate of Lassa virus Concentration in the environment	-0.000
δ_v	Rate of Lassa virus decay from the environment	-1.000
θ_1	Rate of virus shed in the environment by infected humans	0.000
θ_2	Rate of virus shed in the environment by infected rodents	-0.000
q	Efficiency of predation	0.998
a	Half saturation constant	0.428
h	Rodent handling time by humans	-0.907
ξ	Fraction of Symptomatic infectious humans	-0.250
P_2	Rate of predation of Susceptible Rodent by Infected humans	0.999
P_3	Rate of predation of Infected Rodent by Susceptible humans	-0.520
R_0	**Basic reproduction number**	**1.858**

3.4.3. *Comparative analysis of sensitivity results.* Recall that this study approaches the solution of the disease-free state equations by considering two scenarios: one where there is no predation of susceptible rodents (referred to as Case 1) and another where humans actively engage in consuming or preying on susceptible rodents (referred to as Case 2). Consequently, we obtain two distinct disease basic reproduction numbers, each accounting for the respective scenario described above. We also obtain separate sensitivity results for both reproduction numbers. In this section, we investigate how the sensitivity results differ between the two cases. We observe that the two sensitivity results are very similar, as the parameters influencing the reproduction number (R_0) in the first case closely align with those in the second case. However, the parameters corresponding to the migration of rodents (m_1, m_2) are shown to be sensitive in the second case but not in the first case. Migration of susceptible rodents (m_1) is positively related to R_0, whereas the migration of infected rodents (m_2) is negatively related to R_0. Overall, our comparative analysis reveals remarkable consistency between the sensitivity results for the two scenarios.

4. Numerical Analysis and Discussion

To illustrate the theoretical findings, we present the numerical analysis result of the model in this section. Following the results of the sensitivity analysis, we investigate the effect of key parameters on the infected human and rodent populations, as well as the reproduction number. The system described by equations (2a) – (2f) is integrated using the *odeint* function in the Python programming language and simulated under a set of initial values and parameter values in Table 5. We did not align the study with any specific country, so the parameter values were generated from the literature. As a result, we used these values to establish the initial conditions or values for state variables.

Figure 4 illustrates a disease-free state where no virus or Lassa fever is present in the system. This state signifies the absence of infected humans or rodents, resulting in an uninfected environment. In this scenario, there is no recovery in humans, as indicated in Figure 4A, with $I_r = I_h = R_h = V = 0$, while S_r and S_h remain nonzero. Figures 4B and 4C demonstrate that the susceptible human and rodent populations continue to grow rapidly in the disease-free state. This is consistent with the behaviour of Lassa fever. As one expects, in the absence of infection

and holding all other things constant, both human and rodent populations will continue to grow exponentially.

In Figure 5, we present the numerical results of the model simulations for different parameters in the infected human population. Notably, in Figure 5A, the results show that the fraction of the infected human population is characterised by an exponential rise as we increase the rate of rodent contact with the infested environment (β_1). This occurs because increased contact can lead to more infected rodents, as susceptible rodents are exposed to the Lassa virus deposited in the environment [36, 37]. Consequently, humans may have frequent contact with infected rodents, resulting in a high number of human infections.

Furthermore, as depicted in Figure 5B, an increase in the rate of virus deposition into the environment by humans (θ_1) results in a gradual rise in the fraction of the infected human population. This observation underscores the role of human activities in contributing to transmission dynamics. The findings highlight the importance of understanding and controlling factors related to rodent contact and virus deposition to effectively manage the spread of Lassa fever.

In Figure 5C, we explore the impact of human-to-human transmission (β_h) on the infected human population. A reduction in the human-to-human transmission rate can result in a significant decrease in the number of infected individuals. Notably, infected cases emerge only when β_h surpasses a critical threshold, below which the disease remains in an endemic state. This emphasises that maintaining the transmission rate below 50% is crucial for minimising the burden of the disease. This observation aligns with the findings of a prior study conducted by [11], which also demonstrated a correlation between β_h and the dynamics of infected individuals. The consistency between our results and those of [11] underscores the pivotal role of this parameter in the surge of Lassa fever cases. Consequently, efforts to reduce person-to-person contact become paramount in controlling the spread of the disease. These implications are particularly relevant in hospital settings, where nosocomial outbreaks of Lassa fever have been documented [38]. Encouraging measures to minimise direct contact with infectious individuals, especially in healthcare environments, is imperative to curb the risk of outbreaks and protect both patients and healthcare workers.

While in Figure 5D, an increase in the rate of virus decay in the environment (δ_v) leads to a reduction in human infections. Thus, a higher decay rate means less virus in the environment, reducing the frequency of contact between humans or rodents and the virus. Consequently, transmission through the environment diminishes, resulting in a significant decrease in human infections. This result is consistent with the findings of [11], who observed similar influence and therefore suggested that efforts should be targeted at eradicating LASV from the environment by disinfecting surfaces.

In Figure 6A, we observe a rapid increase in the number of individuals infected with Lassa fever when the disease-induced death rate (δ_h) is initially set to zero. This swift rise reaches its peak at time 13 and then starts to gradually decrease. What's particularly noteworthy is that, as we examine the impact of different rates of Lassa fever-induced death, the infected population undergoes a reduction, eventually stabilising into an endemic state within the overall population.

In Figure 6B, we examine the impact of predation, where susceptible humans prey on susceptible rodents, on the dynamics of the infected population. The plot illustrates an initial rapid rise, reaching maximum values, and then a decline to a relative equilibrium in the infected human population. This pattern is likely due to the complex interplay between human behaviour, rodent population dynamics, and the transmission dynamics of the virus. The initial surge is linked to heightened human predation on rodents, creating a greater risk of virus transmission due to the challenge of visually discerning between infected and uninfected rodents. However, the subsequent decline stems from a decrease in the population of susceptible rodents. This reduction results in a decline in the spread of the virus, establishing a more balanced scenario within the infected human population.

Moving on to Figure 6C, we investigate how human infections evolve in response to variations in the rate of rodent migration out of human settlements. Generally, we observe an exponential increase in the infected human population as we decrease the migration rate. For instance, the disease-infected human population stabilises as the migration rate approaches zero. Conversely, the infected human population drastically declines as the rodent migration rate increases. Infections became endemic in the population when the migration rate surpassed 50%.

TABLE 5. System parameters and their values

Parameter	Description	Value	Reference
Λ_h	Rate of recruitment into the human population	0.15	[39, 40]
b	Rate of recruitment into the rodent population	0.172	[39]
k	Environmental carrying capacity for rodents	20000	Assumed
β_r	Disease transmission rate in rodents	0.0553	[12]
β_h	Human-to-human transmission rate	0.1479	[12]
β_1	Rodent contact rate with the infested environment	0.1212	[11]
β_2	Human contact rate with the infested environment	0.0200	[11]
δ_h	Disease-induced death rate in humans	0.0024	[41]
μ_r	Natural death rate in rodents	0.00200	[12]
μ_h	Natural death rate in humans	0.02	[16, 42]
γ_h	Recovery rate of infected humans	0.0236	[12]
ω	Transition from recovered to susceptible	1.5736	[12]
m_1	Rate of migration by susceptible rodents	0.3333	Assumed
m_2	Rate of migration by infected rodents	0.1666	Assumed
η	Rate of Lassa virus concentration in the environment	0.0913	[11]
θ_1	Rate of virus shed in the environment by infected humans	0.0913	[11]
θ_2	Rate of virus shed in the environment by infected rodents	0.4136	[11]
δ_V	Rate of Lassa virus decay from the environment	0.4353	[11]
q	Efficiency of predation	1.0000	Assumed
a	Half saturation constant	1.0000	Assumed
h	Rodent handling time by humans	1.0000	Assumed
P_1	Rate of predation of susceptible rodents by susceptible humans	1.0000	Assumed
P_2	Rate of predation of susceptible rodents by infected humans	1.0000	Assumed
P_3	Rate of predation of infected rodents by susceptible humans	1.0000	Assumed
P_4	Rate of predation of infected rodents by infected humans	1.0000	Assumed

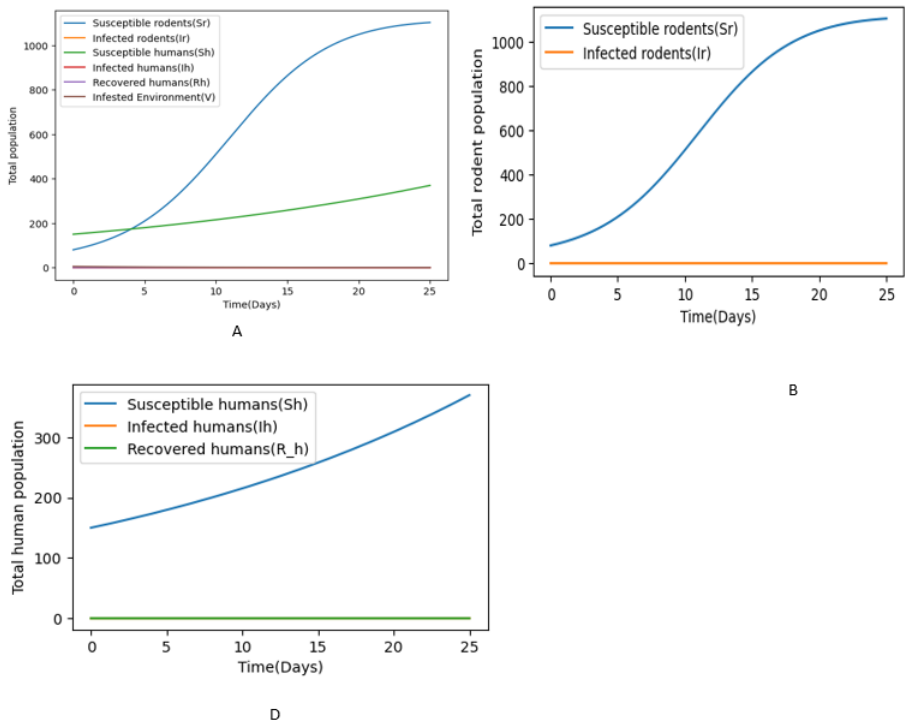

FIGURE 4. Plot illustrating the disease-free equilibrium state of our system.

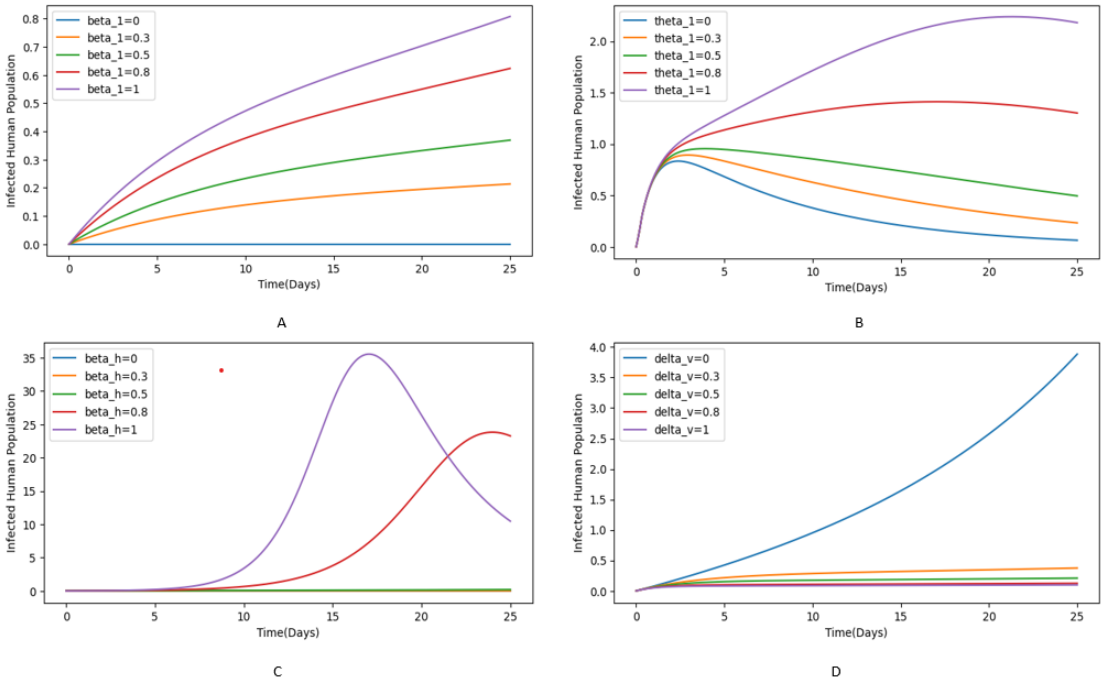

FIGURE 5. Plot illustrating scenario analysis for system parameters.

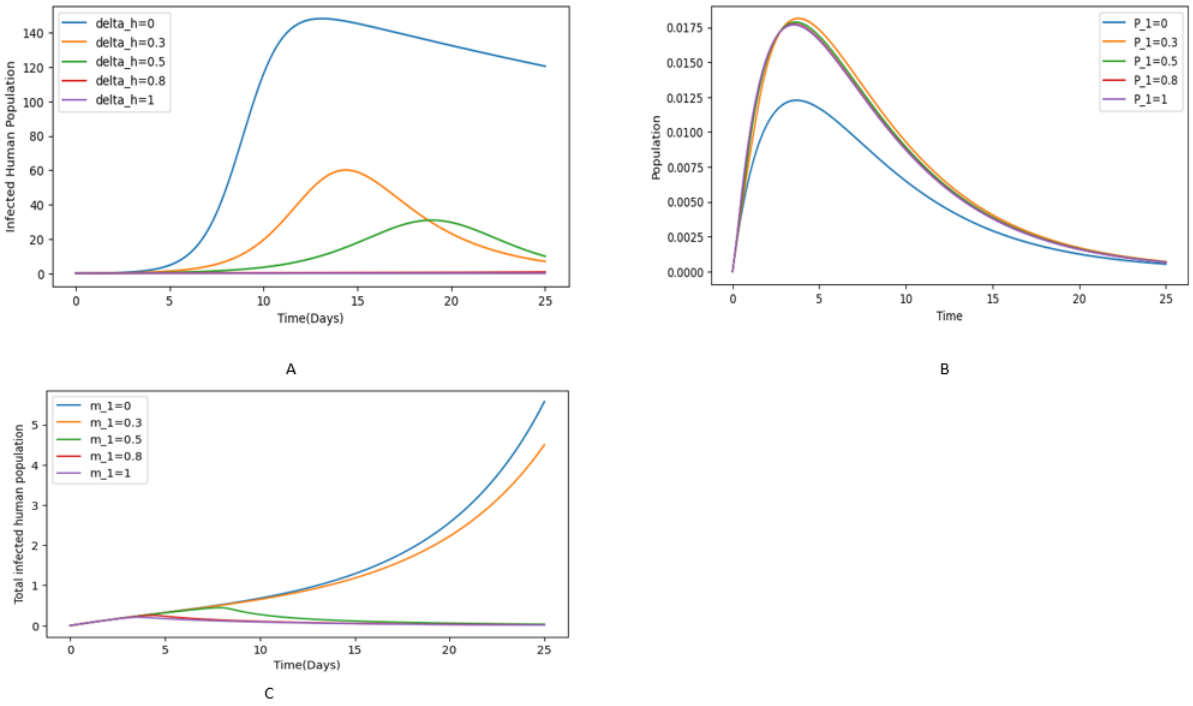

FIGURE 6. Plot illustrating scenario analysis for system parameters on infected human population

5. CONCLUSION

In this study, we develop a five-compartmental mathematical model to elucidate the transmission dynamics of Lassa fever between two interacting populations: rodents and humans. Our model incorporates an infested environment, rodent predation and migration of rodents. The explicit modelling of the predation of rodents (prey) by humans (predators) was achieved through the application of the Holling type II function response. The model, described by systems of non-linear differential equations, underwent comprehensive analytical and numerical analyses to offer insights into the transmission of LF and the influence of various system parameters. We establish our model's mathematical significance, validity, and biological relevance by proving the boundedness, positivity, and existence of solutions. Additionally, we explore the Lassa-free equilibrium by deriving an explicit formula for the basic reproduction number (R_0) using the next-generation matrix method. The introduction of the functional response added complexity to the analysis, prompting an analysis of the Lassa fever-free equilibrium and basic reproduction across three primary cases: (1) no consumption or predation of rodents (no preying); (2)

inefficient human predation on rodents with minimal impact on the rodent-human relationship (useless preying); and (3) active consumption or predation of rodents by humans (useful preying). Our analysis yields distinct reproduction numbers for each case, with a specific focus on scenarios involving no preying (referred to as Case 1) and useful preying (referred to as Case 2). From the baseline parameter values obtained from the literature, we obtained the reproduction numbers for Case 1 as $R_0 = 2.163$ and Case 2 as $R_0 = 1.858$.

Furthermore, a sensitivity analysis result reveals that the rate of predation of infected rodents by susceptible humans (P_3), the handling time of rodents (h), the virus decay rate (δ_v), the recovery rate of humans (γ_h), the human recruitment rate (Λ_h), the disease-induced death rate (δ_h), the predation of susceptible rodents by infected humans (P_2), the saturation constant (a) and the migration rate of rodents are highly sensitive to R_0. Building on these results, numerical analyses were performed to visualise our analytical findings. The study suggests that human-to-human contact (β_h) drives infections in humans when the contact rate exceeds a threshold of 50%. Migration of susceptible rodents (m_1) was observed to drive infections in human populations, and to some extent, rodent predation contributes to an increase in human infections. Consequently, strategies aiming at minimising human contact, reducing rodent presence in human abodes, and mitigating rodent predation are recommended. Moreover, our research stressed the importance of environmental control and surface disinfection in reducing and delaying infection peaks. It is also recommended that individuals in close contact with Lassa fever-infected individuals adopt precautionary measures to mitigate the transmission rate. Given the identified correlation between increased rodent migration and a surge in infections, promoting hygiene practices and discouraging behaviours that encourage rodents to move into human settlements is crucial.

5.1. Limitations and Prospects. Our findings are part of ongoing research and investigations on Lassa fever (LF) disease, and they contribute new insights into the transmission dynamics of the disease. However, our model has limitations. The full transmission dynamics of the disease, including asymptomatic and symptomatic compartments and a death compartment, were not captured. By excluding these key components, the model oversimplifies the actual transmission dynamics of Lassa fever, leading to potentially inaccurate predictions. Consequently, the

model's disease spread and impact predictions may be skewed, leading to misleading conclusions. Additionally, we assumed that all parameters of the model are constant. However, these factors are likely to fluctuate seasonally and over time, significantly influencing Lassa fever's transmission dynamics. Ignoring these variations can lead to misleading conclusions.

Looking ahead, we intend to integrate real-world outbreak data to compare our model's predictions with observed outcomes. This comparison will not only validate the model but also provide a stronger argument for its application in public health strategies. Furthermore, future work could extend these models by incorporating additional layers of complexity, such as spatial dynamics or more detailed age-structured models. Finally, we recommend that future studies capture the full transmission dynamics of Lassa fever to achieve a more nuanced and comprehensive understanding of the disease burden.

ACKNOWLEDGEMENTS

The authors would like to thank the European and Developing Countries Clinical Trials Partnership (EDCTP) for the generous financial support provided to the first author throughout her two years of master's training under the TEBWA program (Training Epidemiologists and Biostatisticians for Enhanced Response to Disease Outbreaks and Epidemics in West Africa), grant number CSA2020E-3131.

CONFLICT OF INTERESTS

The authors declare that there is no conflict of interests.

REFERENCES

[1] Africa CDC, Lassa fever, https://africacdc.org/disease/lassa-fever, Accessed on November 11, 2023.

[2] M.S. Mehand, F. Al-Shorbaji, P. Millett, et al. The WHO R&D Blueprint: 2018 review of emerging infectious diseases requiring urgent research and development efforts, Antiviral Res. 159 (2018), 63–67. https://doi.org/10.1016/j.antiviral.2018.09.009.

[3] J.B. McCormick, I.J. King, P.A. Webb, et al. A case-control study of the clinical diagnosis and course of Lassa fever, J. Infect. Dis. 155 (1987), 445–455. https://doi.org/10.1093/infdis/155.3.445.

[4] A.J. Basinski, E. Fichet-Calvet, A.R. Sjodin, et al. Bridging the gap: Using reservoir ecology and human serosurveys to estimate Lassa virus spillover in West Africa, PLoS Comput. Biol. 17 (2021), e1008811. https://doi.org/10.1371/journal.pcbi.1008811.

[5] O. Ogbu, E. Ajuluchukwu, C.J. Uneke, et al. Lassa fever in West African sub-region: an overview, J. Vect. Borne Dis. 44 (2007), 1–11.

[6] CDC, Prevention Lassa fever fact sheet, (2023). https://stacks.cdc.gov/view/cdc/12236.

[7] A. Abdulhamid, N. Hussaini, S.S. Musa, et al. Mathematical analysis of Lassa fever epidemic with effects of environmental transmission, Results Phys. 35 (2022), 105335. https://doi.org/10.1016/j.rinp.2022.105335.

[8] A. Abidemi, K.M. Owolabi, E. Pindza, Modelling the transmission dynamics of Lassa fever with nonlinear incidence rate and vertical transmission, Physica A: Stat. Mech. Appl. 597 (2022), 127259. https://doi.org/10.1016/j.physa.2022.127259.

[9] M.O. Akinade, A.S. Afolabi, Sensitivity and stability analyses of a lassa fever disease model with control strategies, IOSR J. Math. 16 (2020), 29–42.

[10] W. Atokolo, R.O. Aja, D. Omale, et al. Fractional mathematical model for the transmission dynamics and control of Lassa fever, Franklin Open 7 (2024), 100110. https://doi.org/10.1016/j.fraope.2024.100110.

[11] J.P. Ndenda, J.B.H. Njagarah, S. Shaw, Influence of environmental viral load, interpersonal contact and infected rodents on Lassa fever transmission dynamics: Perspectives from fractional-order dynamic modelling, AIMS Math. 7 (2022), 8975–9002. https://doi.org/10.3934/math.2022500.

[12] M.M. Ojo, B. Gbadamosi, T.O. Benson, et al. Modeling the dynamics of Lassa fever in Nigeria, J. Egypt. Math. Soc. 29 (2021), 16. https://doi.org/10.1186/s42787-021-00124-9.

[13] S. Aloke, P. Okpara, A mathematical model of Lassa fever transmission and control in Ebonyi State, Nigeria, Amer. J. Appl. Math. 12 (2024), 24–36. https://doi.org/10.11648/j.ajam.20241202.11.

[14] J.I. Nchom, A.S. Abubakar, F.O. Arimoro, et al. The role of weather in the spread of Lassa fever in parts of Northern Nigeria, Int. J. Trop. Dis. Health 42 (2021), 33–40. https://doi.org/10.9734/ijtdh/2021/v42i2330562.

[15] P.G.U. Madueme, F. Chirove, Understanding the transmission pathways of Lassa fever: A mathematical modeling approach, Infect. Dis. Model. 8 (2023), 27–57. https://doi.org/10.1016/j.idm.2022.11.010.

[16] T. Faniran, E. Ayoola, Investigating essential factors in the spread of lassa fever dynamics through sensitivity analysis, Int. J. Nonlinear Anal. Appl. 13 (2022), 485–497. https://doi.org/10.22075/ijnaa.2021.22707.2405.

[17] A. Raza, E. Rocha, E. Fadhal, et al. The effect of delay techniques on a lassa fever epidemic model, Complexity 2024 (2024), 2075354. https://doi.org/10.1155/2024/2075354.

[18] F.A. Basir, P.K. Tiwari, S. Samanta, Effects of incubation and gestation periods in a prey–predator model with infection in prey, Math. Computers Simul. 190 (2021), 449–473. https://doi.org/10.1016/j.matcom.2021.05.035.

[19] S. Barua, A. Dénes, M.A. Ibrahim, A seasonal model to assess intervention strategies for preventing periodic recurrence of Lassa fever, Heliyon 7 (2021), e07760. https://doi.org/10.1016/j.heliyon.2021.e07760.

[20] E. Fichet-Calvet, D.J. Rogers, Risk maps of lassa fever in West Africa, PLoS Negl. Trop. Dis. 3 (2009), e388. https://doi.org/10.1371/journal.pntd.0000388.

[21] A.R. Akhmetzhanov, Y. Asai, H. Nishiura, Quantifying the seasonal drivers of transmission for Lassa fever in Nigeria, Phil. Trans. R. Soc. B 374 (2019), 20180268. https://doi.org/10.1098/rstb.2018.0268.

[22] J. Mariën, F. Kourouma, N. Magassouba, et al. Movement patterns of small rodents in lassa fever-endemic villages in Guinea, EcoHealth 15 (2018), 348–359. https://doi.org/10.1007/s10393-018-1331-8.

[23] J. Clark, L. Yakob, M. Douno, et al. Domestic risk factors for increased rodent abundance in a Lassa fever endemic region of rural Upper Guinea, Sci. Rep. 11 (2021), 20698. https://doi.org/10.1038/s41598-021-00113-z.

[24] WHO, Lassa fever fact sheet, 2021. https://www.who.int/news-room/fact-sheets/detail/lassa-fever, Accessed on 24 March 2023.

[25] C.S. Bornaa, O.D. Makinde, I.Y. Seini, Eco-Epidemiological model and optimal control of disease transmission between humans and animals, Commun. Math. Biol. Neurosci. 2015 (2015), 26.

[26] S. Kant, V. Kumar, Analysis of an eco-epidemiological model with migrating and refuging prey, in: P.N. Agrawal, R.N. Mohapatra, U. Singh, H.M. Srivastava (Eds.), Mathematical Analysis and Its Applications, Springer India, New Delhi, 2015: pp. 17–36. https://doi.org/10.1007/978-81-322-2485-3_2.

[27] A. Savadogo, B. Sangaré, H. Ouedraogo, A mathematical analysis of Hopf-bifurcation in a prey-predator model with nonlinear functional response, Adv. Differ. Equ. 2021 (2021), 275. https://doi.org/10.1186/s13662-021-03437-2.

[28] C. Maji, D. Mukherjee, D. Kesh, Deterministic and stochastic analysis of an eco-epidemiological model, J. Biol. Phys. 44 (2017), 17–36. https://doi.org/10.1007/s10867-017-9472-5.

[29] J. Bonwitt, A.H. Kelly, R. Ansumana, et al. Rat-atouille: a mixed method study to characterize rodent hunting and consumption in the context of lassa fever, EcoHealth 13 (2016), 234–247. https://doi.org/10.1007/s10393-016-1098-8.

[30] M. Douno, E. Asampong, N. Magassouba, et al. Hunting and consumption of rodents by children in the Lassa fever endemic area of Faranah, Guinea, PLoS Negl. Trop. Dis. 15 (2021), e0009212. https://doi.org/10.1371/journal.pntd.0009212.

[31] F. Klawonn, G. Hoffmann, An objective function-based clustering algorithm with a closed-form solution and application to reference interval estimation in laboratory medicine, Algorithms 17 (2024), 143. https://doi.org/10.3390/a17040143.

[32] R. Wituła, D. Słota, Cardano's formula, square roots, Chebyshev polynomials and radicals, J. Math. Anal. Appl. 363 (2010), 639–647. https://doi.org/10.1016/j.jmaa.2009.09.056.

[33] O. Diekmann, J.A.P. Heesterbeek, J.A.J. Metz, On the definition and the computation of the basic reproduction ratio R_0 in models for infectious diseases in heterogeneous populations, J. Math. Biol. 28 (1990), 365–382. https://doi.org/10.1007/bf00178324.

[34] P. van den Driessche, J. Watmough, Reproduction numbers and sub-threshold endemic equilibria for compartmental models of disease transmission, Math. Biosci. 180 (2002), 29–48. https://doi.org/10.1016/s0025-5564(02)00108-6.

[35] M.M. Ojo, E.F.D. Goufo, Modeling, analyzing and simulating the dynamics of Lassa fever in Nigeria, J. Egypt. Math. Soc. 30 (2022), 1. https://doi.org/10.1186/s42787-022-00138-x.

[36] O.S. Obabiyi, A.A. Onifade, Mathematical model for Lassa fever transmission dynamics with variable human and reservoir population, Int. J. Differ. Equ. Appl. 16 (2017), 67–91.

[37] National Institute for Communicable Diseases, Lassa fever, https://www.nicd.ac.za/diseases-a-z-index/lassa-fever, 2020, Retrieved on 2023-12-01.

[38] C.C. Dan-Nwafor, O. Ipadeola, E. Smout, et al. A cluster of nosocomial Lassa fever cases in a tertiary health facility in Nigeria: Description and lessons learned, 2018, Int. J. Infect. Dis. 83 (2019), 88–94. https://doi.org/10.1016/j.ijid.2019.03.030.

[39] F. Akinpelu, R. Akinwande, Mathematical model for lassa fever and sensitivity analysis, J. Sci. Eng. Res. 5 (2018), 1–9.

[40] L.M. Erinle-Ibrahim, O. Adebimpe, W.O. Lawal, et al. A mathematical model and sensitivity analysis of lassa fever with relapse and reinfection rate, Tanzania J. Sci. 48 (2022), 414–426. https://doi.org/10.4314/tjs.v48i2.16.

[41] A.C. Loyinmi, T.K. Akinfe, A.A. Ojo, Qualitative analysis and dynamical behavior of a Lassa haemorrhagic fever model with exposed rodents and saturated incidence rate, Sci. Afr. 14 (2021), e01028. https://doi.org/10.1016/j.sciaf.2021.e01028.

[42] S. Dachollom, C. Madubueze, Mathematical model of the transmission dynamics of Lassa fever infection with controls, Math. Model Appl. 5 (2020), 65–86. https://doi.org/10.11648/j.mma.20200502.13.